

Active-Layer Hydrology in Nonsorted Circle Ecosystems of the Arctic Tundra

Ronald P. Daanen, Debasmita Misra,* and Howard Epstein

Patterned-ground features are common throughout arctic tundra ecosystems and develop as a result of intricate relationships among climate, hydrology, vegetation, and soil processes. Changes in the annual energy budget induced by climatic warming could likely affect the arctic freeze–thaw cycles, altering biogeochemistry and soil processes, which in turn could change the patterned-ground ecosystem. In this study, we concentrate on the hydrology of the nonsorted circle system, an example of arctic tundra patterned ground in a relatively stable condition. Our objective was to model the processes governing liquid water movement in the active layer during freezing in order to identify the driving forces that alter the balance within this system. Our model simulations demonstrate that water redistributes within the active layer during freezing as an indirect result of horizontal differences in soil temperature. Soil surface insulation (such as that imposed by vegetation or snow) causes preferential ice accumulation in adjacent noninsulated areas, which inhibits vegetation from colonizing these areas. Both lower soil freezing rates and increased vegetation on nonsorted circles reduce water movement to the center of these features, potentially altering the equilibrium condition of these systems.

The interdependency of biological and physical components of the arctic tundra system can yield strongly nonlinear processes with potential thresholds for ecosystem shifts. Hydrology critically influences the ecosystem dynamics in the Arctic, even though the tundra appears to have a relatively simple hydrologic system, often consisting of only a saturated active layer underlain by permafrost. Disturbances associated with the freezing and thawing of the active layer (cryoturbation) are key hydrological processes that shape the arctic tundra. In most cases, water is assumed to be present in excess, and its sources are, therefore, mostly ignored. One type of land surface formation generated by active layer freezing and thawing is the nonsorted circle.

Nonsorted circles (sometimes referred to as frost boils) are approximately 1 to 3 m in diameter and generally have little vegetation on them due to excessive soil expansion from ice accu-

mulation during winter (Washburn, 1956). Nonsorted circles are, however, typically surrounded by dense vegetation, which acts as an insulator against winter cooling, leading to preferential formation of ice within the circles. The water needed for the observed ice formation within the circle is thought to migrate horizontally from vegetation-covered soil, outside of the circle, as a result of increased tension within the circle during freezing. Thus, moisture migrates laterally as a result of horizontal differences in insulation at the surface, particularly in fine-textured soils. The detailed processes governing the formation and persistence of nonsorted circles and their effects on soil–plant–water relationships are still an area of active research (Peterson and Krantz, 2003).

Several modeling studies have focused on ice lens formation within nonsorted circles that causes substantial soil expansion (frost heave) (Miller, 1980; Fowler and Krantz, 1994). Yet these and other models account for only a single dimension, which is insufficient to capture the hydrological dynamics of a nonsorted circle (Boike et al., 2002). Nicolosky et al. (2004) developed a two-dimensional model that accurately estimates frost heave for a single nonsorted circle, assuming an open system with an unlimited supply of water. However, even in a relatively saturated arctic tundra system, the available water is limited; therefore, for accurate results, the supply of water generating frost heave must be present within the domain of the simulation. Ippisch (2003) developed a three-dimensional model that also captures the dynamics of a single nonsorted circle; however, the details focus more on gas and solute flow than on the rheology of the soil. The modeling of these systems could be improved to include coupled

R.P. Daanen, Geophysical Institute, Univ. of Alaska Fairbanks, Fairbanks, AK 99775; D. Misra, Geological Engineering, Dep. of Mining and Geological Engineering, College of Engineering and Mines, Univ. of Alaska Fairbanks, Fairbanks, AK 99775; H. Epstein, Dep. of Environmental Sciences, Univ. of Virginia, Charlottesville, VA. Received 27 Nov. 2006. *Corresponding author (ffdm1@uaf.edu).

Vadose Zone J. 6:694–704
doi:10.2136/vzj2006.0173

© Soil Science Society of America
677 S. Segoe Rd. Madison, WI 53711 USA.
All rights reserved. No part of this periodical may be reproduced or transmitted in any form or by any means, electronic or mechanical, including photocopying, recording, or any information storage and retrieval system, without permission in writing from the publisher.

biological and physical processes across a domain larger than just a single nonsorted circle.

Ecosystem changes caused by recent climate warming are apparent in the arctic tundra (Myneni et al., 1997; Jia et al., 2003; Chapin et al., 2005; Tape et al., 2006; Walker et al., 2006), and determining how ecosystem changes affect patterned-ground features and subsequent system feedbacks provides areas of active research (Walker et al., 2004). Climate warming has changed the arctic vegetation quantity and composition (Jia et al., 2003; Walker et al., 2006) and thus has affected the local and regional energy budgets and hydrological processes (Chapin et al., 2005). In this study, we focus on the hydrology of the nonsorted circle system, which is an example of a relatively stable patterned-ground system (Fig. 1). Understanding the active layer hydrology and its relationship with soils and plants in the arctic tundra will help us assess the impact of climate warming on ecosystems in the cold regions.

A key component in maintaining nonsorted circle ecosystems, water is generally abundant in the southern arctic tundra during fall freezing, as most water in the active layer (the surface soil layer that thaws on an annual basis) is a product of snowmelt and thawing soil in the spring and summer. The permafrost below the active layer prevents any vertical drainage, thus creating the potential for inundated soils. Frost heave, the process of soil expansion as a result of ice lens formation during freezing, depends on the presence of water and soil texture. Soil texture allows liquid water to be present at below-freezing temperatures.



FIG. 1. Top: Individual nonsorted circles in the top part of the figure near Franklin Bluffs, AK. Bottom: An aerial view of the patterned ground on Banks Island, NT, Canada (courtesy Biocomplexity Project, UAF).

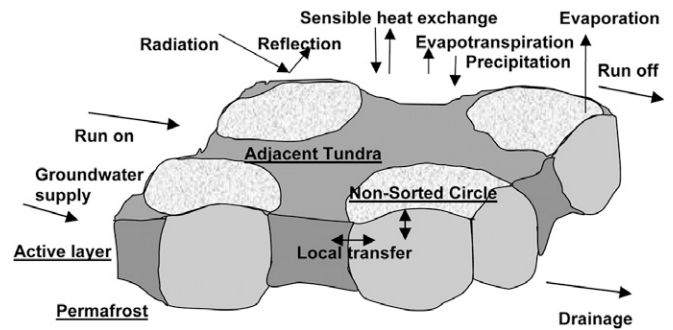


FIG. 2. Schematic of heat and mass transfer fluxes in a typical nonsorted circle ecosystem.

In general, fine-textured soils with relatively high hydraulic conductivities, like silts, are susceptible to frost heave (Mitchell, 1993). Cryoturbation from frost heave prevents vegetation succession in areas that accumulate additional water in the form of ice during the winter. Figure 2 illustrates the typical surface and subsurface fluxes of energy and mass in the nonsorted circle ecosystem.

Surface vegetation and organic matter alter heat flow into and out of the ground. Surface heat fluxes combined with water movement in the soil determines the strength and location of ice accumulation and cryoturbation. Areas with little vegetation within the nonsorted circle system experience more frost heave during the winter than areas with dense vegetation cover (Walker et al., 2004). We conclude from these observations that more ice accumulates in areas with limited insulation at the soil surface.

We investigated the horizontal movement of water resulting from temperature gradients during freezing using a numerical model called Water Ice Temperature (WIT) (Daanen, 2004). The model simulates heat and water flow in porous media, particularly snow (Daanen and Nieber, unpublished data, 2007), and simulates water movement in the active layer and ice accumulation as a result of differential surface insulation. The model combines the laws of heat and mass conservation, heat and water flux, and phase change in a porous medium (Daanen, 2004).

The objective of this study is to identify the driving forces that potentially alter the structure of the nonsorted circle system under a climate change scenario. This was done using the WIT model. Hydrology is critically important in maintaining the local balance of physical, chemical, and biological processes in the nonsorted circle ecosystem and is best illustrated by a simple conceptual model (Fig. 3). In a simplified representation of the system, we consider ice accumulation caused by

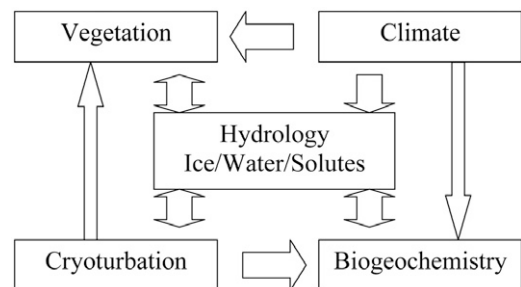


FIG. 3. Conceptual diagram of the hydrology and its relation to other processes in a typical nonsorted circle ecosystem.

temperature gradients, which result from differences in insulation (vegetation, dead organic matter, snow) at and near the soil surface. Climate models predict dramatic changes for the arctic tundra environment, such as shifts in summer and winter temperatures, with enhanced winter precipitation (Maxwell, 1992; Walsh, 1993). This model accounts for current climatic conditions and simulates warmer air temperatures during freezing and increased soil surface insulation resulting from increased snowfall and vegetation.

Model Description

The governing equations involved in nonsorted circle hydrology include the conservation of mass for water and ice, conservation of energy, flux laws for liquid water (Richards' equation) and heat (Fourier's law), and relations of thermodynamic equilibrium (generalized Clapeyron equation). These relationships are strongly dependent on each other and directly coupled in the model. The model uses the van Genuchten (1980) equation to approximate the freezing characteristic curve and the hydraulic conductivity curve. This model is similar to that given by Hansson et al. (2004), but it differs in the linkage between ice content and temperature. The model WIT solves a three-dimensional, variably saturated domain with an Eulerian grid system.

Conservation of Mass Equations

The conservation of mass principles have been applied to two water phases as described for liquid water

$$\frac{\partial(\rho_l \theta_l)}{\partial t} = -\nabla \cdot (\rho_l q_l) + E_{i,l} \quad [1]$$

and for ice

$$\frac{\partial(\rho_i \theta_i)}{\partial t} = -E_{i,l} \quad [2]$$

where ρ_l is liquid density and ρ_i is ice density (kg m^{-3}); θ_l is liquid water content and θ_i is ice content ($\text{m}^3 \text{m}^{-3}$); t is time; q_l ($\text{m}^3 \text{s}^{-1}$) is non-Darcy's type flux for liquid; and $E_{i,l}$ ($\text{kg s}^{-1} \text{m}^{-3}$) is freeze-melt mass transfer. The liquid water content of the system is restricted in the model as follows:

$$\theta_s \geq \theta_l \geq \theta_r \quad [3]$$

where θ_s and θ_r are saturated and residual water content ($\text{m}^3 \text{m}^{-3}$), respectively. However, the ice content (θ_i) is globally limited by the available water in the profile yet is locally unlimited, to account for the flux and accumulation within the nonsorted circle.

The classic way to describe liquid water movement in porous media is by combining Darcy's law and the conservation of mass equation. In unsaturated porous media, with air or ice present in the pores, the combined equation is known as Richards' equation (Richards, 1931):

$$\frac{d\theta_l}{d\psi_m} \frac{\partial \psi_m}{\partial t} = -\nabla \cdot [K(\psi_m) \nabla \psi_m + K(\psi_m) \vec{k}] \quad [4]$$

where ψ_m (m) is matric pressure head, K (m s^{-1}) is unsaturated hydraulic conductivity, and \vec{k} (dimensionless) is gravitation

force, unit vector, which equals 1 downward. The term $d\theta_l/d\psi_m = C$ in Eq. [4] is known as the capacitance and the inverse of the tangent of the water retention relation. In a freezing environment, this relationship is often referred to as the freezing characteristic curve (the amount of liquid water present at a certain freezing temperature of the porous medium). This relationship depends on the pore size and grain packing. In this study, we used the similarity between the freezing characteristic curve and the water retention curve as described by Spaans and Baker (1996) and the soil moisture characteristic relation proposed by van Genuchten (1980):

$$\theta_l = \theta_r + (\theta_s - \theta_r) \left(\frac{1}{|\alpha \psi_m|^n + 1} \right)^m \quad [5]$$

where α (1 m^{-1}), m , and n are van Genuchten parameters, and $m = 1 - (1/n)$.

For our model, we used $\alpha = 0.1$ and $n = 1.6$ because these values are based on (and assumed from) the soil type prevalent in arctic nonsorted circles, such that the model corresponds well with the field data at the most critical temperatures for ice lens formation (-5°C to 0°C), and the hydraulic conductivity is large enough to sustain water migration to the nearest ice lens (Fig. 4). The region in the freezing soil where this occurs is also known as the frozen fringe (O'Neill and Miller, 1985).

We used the general Clapeyron equation to relate the matric pressure head with the temperature for the freezing characteristic curve, assuming an ice pressure head (ψ_i) of zero. This thermodynamic relation is the basis of phase change; it was derived for soils by Kay and Groenevelt (1974) and can be described as

$$\psi_m = \left(\frac{L_f}{273.15 \times g} \right) T + \psi_i \quad [6]$$

where L_f is latent heat of fusion ($0.33\text{E} + 6$ [J kg^{-1}]), g (m s^{-2}) is acceleration of gravity, and T ($^\circ\text{C}$) is temperature. Formation of ice crystals in the pores affects the water retention curve; however, this most likely occurs in coarse-grained materials. Because of the fine-grained soil texture in nonsorted circle areas, we used the same water retention curve for the entire freezing process and assumed that any effect on the curve because of ice crystal formation in the pores to be negligible.

We assumed that ice formation occurred mainly as little veins outside the original pore structure. From this, we then assumed that all of the small pores that contain liquid water are available for liquid water flow. For this study, we assumed a saturated hydraulic conductivity (K_s) of $1.0\text{E}-7$ (m s^{-1}) based on the soil type found at the Franklin Bluffs site on Alaska's north slope (Ping et al., 2004) and without ice present in the soil. We computed the unsaturated hydraulic conductivity in Fig. 4 using the van Genuchten (1980) equation given by

$$K(\theta_l) = K_s \left(\frac{\theta_s - \theta_r}{\theta_l - \theta_r} \right)^{1/2} \left(1 - \left[1 - \left[\left(\frac{\theta_s - \theta_r}{\theta_l - \theta_r} \right)^{1/m} \right] \right]^m \right)^2 \quad [7]$$

where the liquid water content is related to the soil temperature through the general Clapeyron equation and the freezing characteristic function.

Energy Equations

The conservation of energy principle is applied to each of the water phases and the soil solid phase. The resulting conservation equations are provided for liquid water,

$$C_v^l \frac{\partial T_l}{\partial t} = -\nabla \cdot q_h^l + Q_h^{i,l} \quad [8]$$

ice,

$$C_v^i \frac{\partial T_i}{\partial t} = -\nabla \cdot q_h^i - Q_h^{i,l} - L_{\tau} E_{i,l} \quad [9]$$

and soil:

$$C_v^s \frac{\partial T_s}{\partial t} = -\nabla \cdot q_h^s \quad [10]$$

where C_v^l , C_v^i , and C_v^s ($J \text{ } ^\circ\text{C}^{-1} \text{ m}^{-3}$) are volumetric heat capacity of the liquid phase, ice, and soil; T_l , T_i , and T_s ($^\circ\text{C}$) are temperature of liquid, ice, and soil; q_h^l , q_h^i , and q_h^s ($J \text{ s}^{-1}$) are Darcy's type sensible heat flux in liquid, ice, and dry soil; and $Q_h^{i,l}$ ($J \text{ s}^{-1} \text{ m}^{-3}$) is sensible heat exchange between liquid and ice. Under local thermal equilibrium conditions ($T_l = T_i = T_s$), the bulk heat conservation equation is obtained by combining Eq. [8–10] as

$$\frac{\partial(C_v T)}{\partial t} = -\nabla q_h - L_{\tau} E_{i,l} \quad [11]$$

where q_h is the vector sum given as

$$q_h = q_h^l + q_h^i + q_h^s \quad [12]$$

The heat flux consists of three major components: conduction through the soil matrix, conductance through ice, and convection with the liquid water flow. The heat flux is a function of the temperature gradient and mass fluxes for convection of heat. This heat flux is given by

$$q_h = -\lambda \nabla T + (C_l \rho_l q_l) \Delta T \quad [13]$$

where C_l ($J \text{ kg}^{-1} \text{ } ^\circ\text{C}^{-1}$) is the specific heat of liquid water and the thermal conductivity, λ ($J \text{ s}^{-1} \text{ m}^{-1} \text{ } ^\circ\text{C}^{-1}$), is assumed to be a function of the porosity and ice content. We parameterized the equation to fit the measured data using the following relationship for estimating λ :

$$\lambda = K_{T_s} * (1 - \theta_s) + \theta_i * K_{T_i}, \quad [14]$$

where $K_{T_s} = 0.7 J \text{ s}^{-1} \text{ m}^{-1} \text{ } ^\circ\text{C}^{-1}$ represents the thermal conductivity of the unfrozen soil (mineral and organic) and $K_{T_i} = 2.1 J \text{ s}^{-1} \text{ m}^{-1} \text{ } ^\circ\text{C}^{-1}$ represents the additional thermal conductivity due to ice in the soil. We found these values through trial and error; they do resemble the thermal conductivities found in the area using inverse modeling techniques.

The combination of heat and mass transfer in unsaturated porous media exposed to freezing conditions has been developed before (Kay and Groenevelt, 1974; Kung and Steenhuis, 1986; Hansson et al., 2004). Kung and Steenhuis (1986) derived a model for coupled heat and mass transfer in freezing soils, but their solution included vapor as an integral part of the solution,

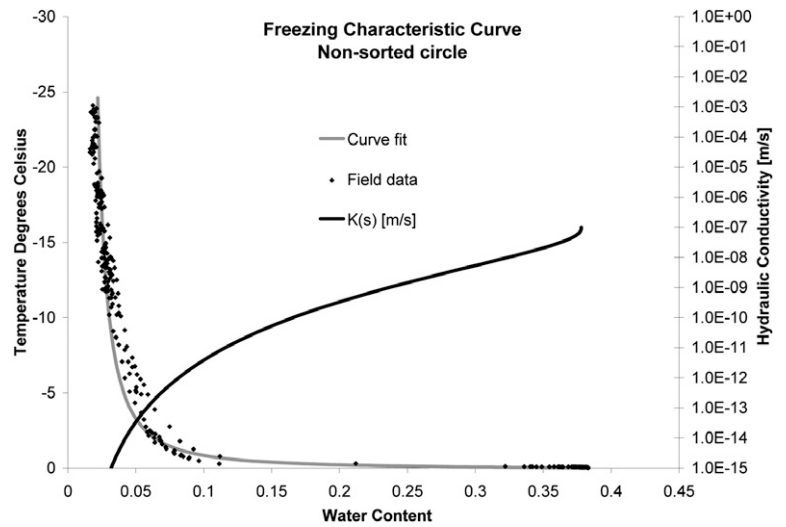


FIG. 4. Measured soil volumetric liquid water content (v/v) versus temperature and fitted freezing characteristic curve using the combination of the van Genuchten (1980) equation and the general Clapeyron relation.

which may be ignored in near-saturated soils, to minimize computation time. Hansson et al. (2004) provided soil column measurements and described a model that is similar to the model presented in this paper.

Figure 5 shows the measured data from Hansson et al. (2004) with simulated results from WIT. We discretized the domain with 1-cm grid spacing.

Similar to Hansson et al. (2004), we found that the lower boundary condition is not completely zero flux. We set the lower boundary to a fixed temperature of 6°C and found a close agreement. Differences between the observed and simulated total water contents could be due to an overestimation of the hydraulic conductivity close to the freezing front; our model does not have an impedance factor discussed by Hansson et al. (2004).

Numerical Solution Procedure

We substituted and discretized the unsaturated freezing soil equations presented above in three dimensions and solved numerically for the temperature and ice content; we used a mid-point finite difference numerical approach (also known as mixed finite element approach [Misra, 1994]) to solve this highly nonlinear system of equations. We accomplished the linearization through a mass conservative solution of the Picard approximation (Celia et al., 1990), and reduced the linear solution matrix with the block Jacobi method. We assumed that horizontal fluxes are constant within the linear matrix solution (a requirement) and solved the resultant banded matrix directly for all vertical nodes stacked on each other. The iterations we conducted for the nonlinearity also provided an opportunity to update the horizontal fluxes, since they were assumed constant during the solution of the matrix with the block Jacobi method. Updating all fluxes within the iteration procedure guaranteed a fully implicit solution of the equations. For this model, it turned out that this numerical approach of the equations was the fastest, or the least expensive, way of solving them implicitly for a large domain in three dimensions.

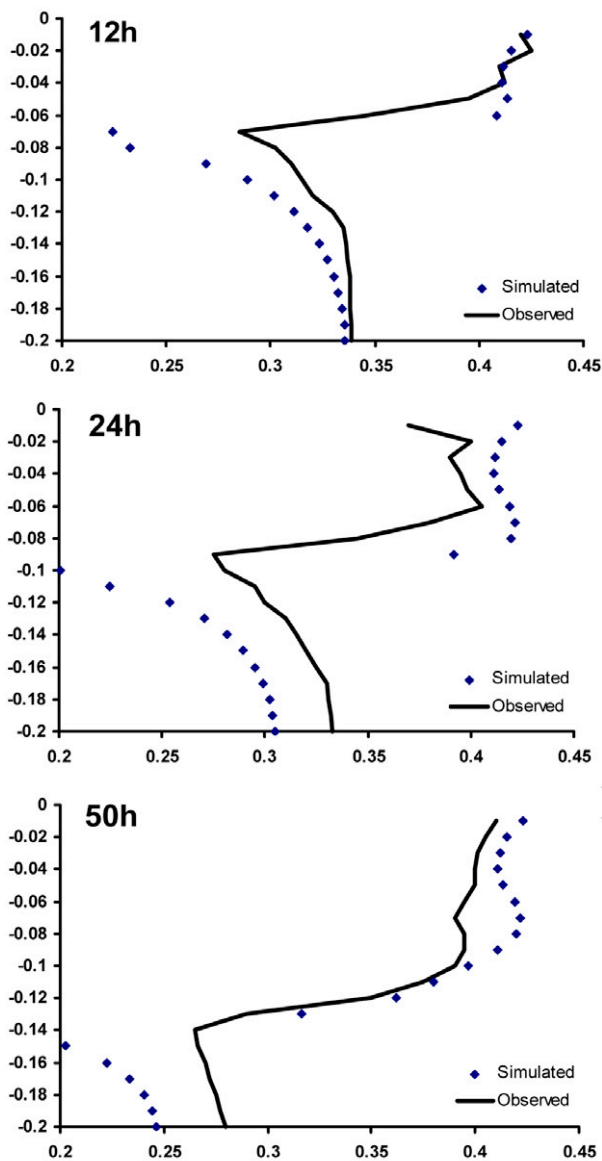


FIG. 5. Model verification with data obtained from Hansson et al. (2004). The y-axis represents the distance from the top of the column (m), and the x-axis represents the volumetric moisture content (v/v).

Boundary and Initial Conditions

The boundary conditions for this model are important for the prediction of ice accumulation in particular areas. Most active layer processes of the arctic tundra are driven by the upper boundary. For this study, we considered a 3- × 3-m uniform area without any gradients that represented the arctic tundra with zero-flux side boundaries for heat as well as water. We also defined a zero water flux for the lower and upper boundaries. We performed the simulation using a depth of 1.7 m. We discretized the vertical and horizontal domain by 10 cm for the upper seven nodes in each column and 1 m × 10 cm × 10 cm for the lowest node to represent the permafrost underlying the active layer. To calibrate and test the WIT model, we used a fixed upper boundary, which was partially insulated and partially exposed to the atmosphere, representing the adjacent tundra and the nonsorted circle, respectively. In this study, we used a single value for representative insulation of the adjacent tundra soil surface, even

though the actual insulation is more complex due to layers of vegetation, dead organic matter, and snow cover.

We solved the soil surface temperature iteratively by assuming that the heat conduction between the air and the mineral soil surface, through the vegetation, organic layer, and snow, is equal to the heat conduction between the soil surface and the first solution node below the surface (Liebethal and Foken, 2007). We calculated the fluxes using the R-value for insulation properties, the air temperature and the upper temperature from the solution domain. The R-value is defined as the inverse of the convective heat transfer coefficient as described by Hansson et al. (2004). The R-value ($\text{m}^2 \text{s } ^\circ\text{C J}^{-1}$) is related to the thickness and thermal conductivity of the surface layer:

$$R = d_{\text{sur}} / \lambda_{\text{sur}} \quad [15]$$

where d_{sur} (m) is the depth of the surface layer and λ_{sur} ($\text{J s}^{-1} \text{m}^{-1} \text{ } ^\circ\text{C}^{-1}$) is the bulk thermal conductivity of the surface. We selected the R-value of the boundary layer to reflect a combination of heat transfer limiting factors such as reduced air movement in the vegetation, snow, and organic layer all lumped into a single parameter, as mentioned above. We assumed the lower boundary temperature at a depth of 1.7 m to be constant at -1.0°C to correspond to field measured data. We assumed the thermal conductivity of the lower boundary to be $2.0 \text{ J s}^{-1} \text{m}^{-1} \text{ } ^\circ\text{C}^{-1}$, which represents an ice-rich mineral medium. In addition to the lower boundary heat flux calculation, we increased the size (1 m) of the lowest node of the domain to serve as a buffer for heat storage at the lower boundary, to aid the modeling accuracy and to suppress any numerical dispersion due to the solution of the heat balance equation. We specified the initial conditions for the model as the liquid water content, the ice content, and the temperature throughout the solution domain. These three components were brought to equilibrium using conservation of mass and energy. Temperature was related to the liquid-water pressure head through the general Clapeyron equation with the use of the moisture characteristic curve; the liquid-water content and the medium temperature were recalculated to match local equilibrium for the initial condition.

Results and Discussion

We simulated only the freezing portion of the annual cycle, with the model calibrated using field data from an arctic tundra site near Franklin Bluffs on the North Slope, Alaska (for more information on this site, see Walker et al., 2004). We used WIT to determine the effects of increased air temperature and surface insulation changes on the horizontal water movement during freezing. We used field temperature and liquid water content data (Daanen, Marchenko, Romanovsky, and Walker, unpublished data, 2007) to calibrate the water retention curve to the mineral soil. Figures 4 and 6 show the freezing characteristic curves used in this study. We measured liquid water content with time domain reflectometry and the soil temperature with a thermistor. This curve (Fig. 4) fits well for areas with very high hydraulic conductivity during freezing, which is important for ice-lens formation. Organic matter buildup beneath the vegetation has altered the original mineral properties of the adjacent tundra soils, as is evident from Fig. 6.

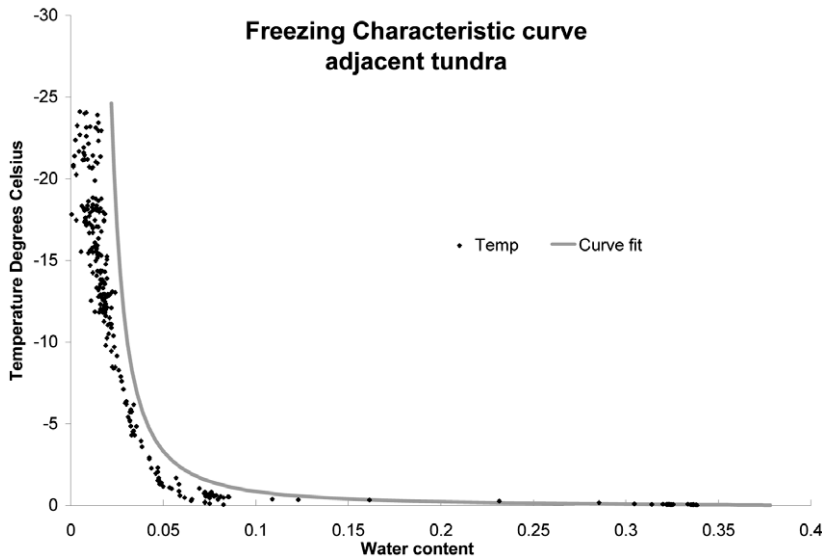


FIG. 6. Freezing characteristic data for the adjacent tundra. The curve used in the plot is the same as in Fig. 4, measured soil volumetric water content (v/v) versus temperature and fitted freezing characteristic curve, fitted to the nonsorted circle data. This figure expresses the difference in soil character for the nonsorted circle and adjacent tundra. The field data was obtained from the location of 1.0×1.0 m in our simulation grid.

We used measured soil temperatures from the nonsorted circle and adjacent tundra at 10-cm intervals from 5 cm below the surface up to 95 cm depth. We used data from four soil-temperature profile probes placed on a line in the field from the nonsorted circle to the adjacent tundra and calibrated the model with the measured air temperature from the site (Fig. 7).

Our solution domain encloses an area that includes the measured data points for the nonsorted circle and the adjacent tundra. Figure 8 shows the results of the calibration for the ice content distribution in the top soil layer. Figure 9 shows the soil temperature, and Fig. 10 illustrates the degree of fit of our model for the measured versus calculated soil temperatures. The ice content distribution (Fig. 8) shows that the liquid water redistributed during freezing in the direction of the arrows. The R -values ($\text{m}^2 \text{s } ^\circ\text{C } \text{J}^{-1}$) at the soil surface follow a sinusoidal curve on the y and x axes, resulting in a high insulation value (6.7) in the

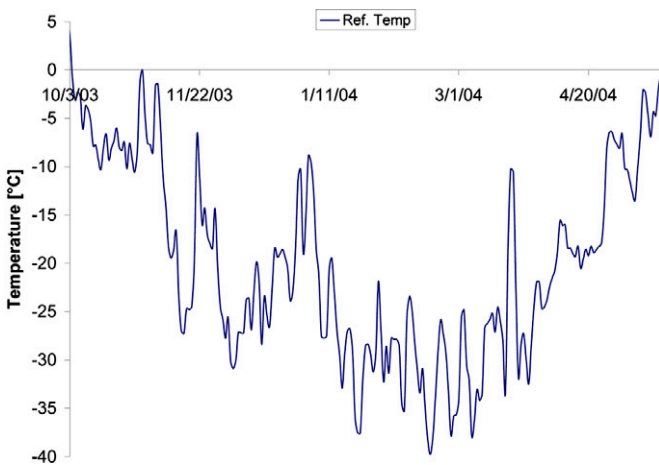


FIG. 7. Air temperatures for the Franklin Bluffs site as input for the simulation model.

lower left-hand side (near coordinate 10×10) and a low insulation value (2.0) in the upper right-hand side (near coordinate 23×23). These results demonstrate that the area with the least amount of surface insulation (the upper right-hand side) obtains the greatest amount of ice accumulation. We found these R -values during model calibration with respect to observed soil temperatures and later realized that they correspond closely with measured values from the nonsorted circle ecosystem near Franklin Bluffs (Daanen, Misra, Epstein, and Walker, unpublished data, 2007).

The simulated soil-temperature data (Fig. 9) show a close fit to the field data except for errors, such as the underestimation of the freezing temperature in the adjacent tundra at 25 cm, that may attribute to temporal variation of snow depth over the winter, which was not taken into account by the model, and spatial variability of vegetation in smaller detail. The constant snow depth in the model results in an underprediction of soil temperature in the fall and an overprediction of soil temperature at the end of winter.

We calibrated this model with soil temperatures from a nonsorted circle and adjacent tundra environment. For future use, the model will have to be tuned to account for the temporal variations in the upper boundary caused by the snow depth at the surface.

At this point, we lack a dynamic snowpack regime in our model that can handle the three-dimensional effects of snow and incorporate vegetation variation at the soil surface. The ice content plot in Fig. 8 shows the movement of the liquid water from the adjacent area toward the nonsorted circle, which matches the

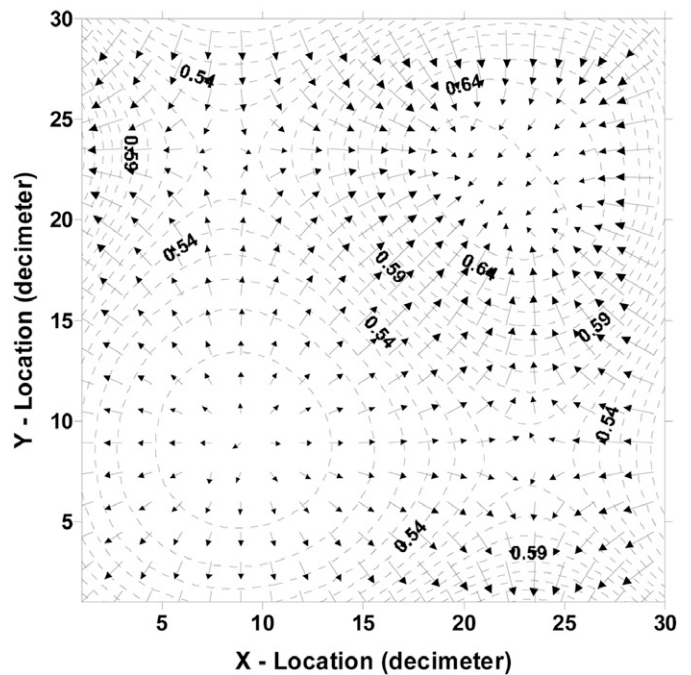


FIG. 8. Overview of the simulation area showing the ice content distribution at a depth of 5 cm as obtained from the numerical model WIT. The arrows represent the direction of the liquid water movement.

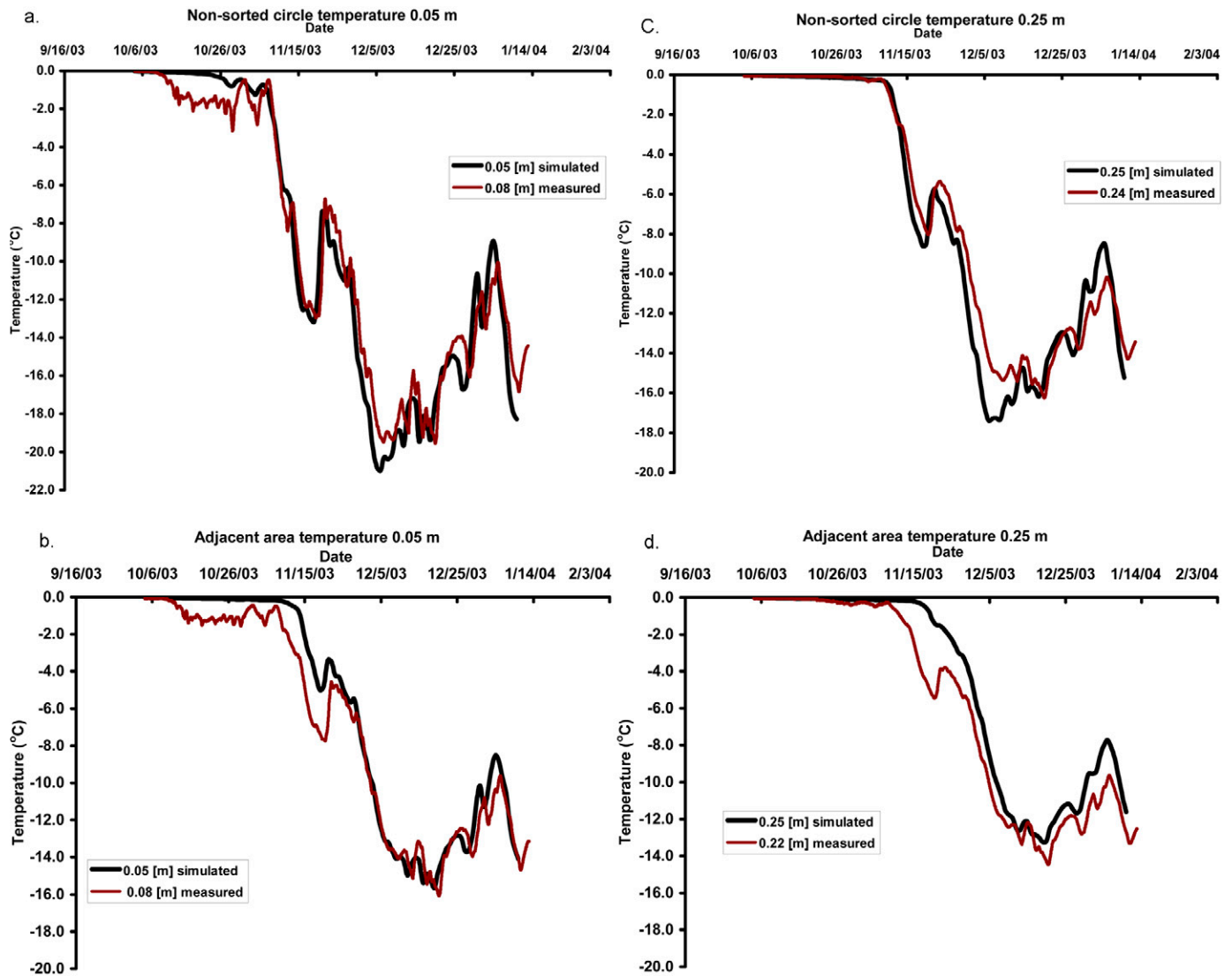


FIG. 9. Soil temperature comparison of measured data and simulated results (a) at 5 cm depth in a nonsorted circle, (b) at 5 cm depth in the adjacent tundra, (c) at 25 cm depth in a nonsorted circle, and (d) at 25 cm depth in the adjacent tundra.

observations that differential heave is present in the nonsorted circle environment. These results agree qualitatively with field observations during any particular freezing season.

The horizontal liquid water flux during freezing indicates the potential for differential frost heave. The water that enters the nonsorted circle from the adjacent tundra area is the horizontal liquid flux. This flux is expressed as centimeters of liquid water over the simulation period. For this study, we used the column at 23×23 to evaluate this flux.

Soil heave occurs when liquid water freezes and expands; subsequent water movement causes extended heave (secondary frost heave) in sparsely vegetated areas. The formation of distinct ice lenses between soil particles (segregated ice) causes secondary frost heave. Primary frost heave accounts for 9% of the liquid water expansion in the pores. If the active layer were 1 m deep with a 40% saturated porosity then the frost heave would be only 3.6 cm, more or less equal for the nonsorted circles as for the adjacent tundra.

For the calibrated domain, we obtained 1.03 cm of horizontal liquid-water flow (corresponding to a potential amount

of segregated ice of 1.12 cm) at the nonsorted circle location (2.3×2.3 m). Assuming that the adjacent tundra heaves at its 9% expansion, the differential heave would be 2.24 cm. This value is small compared with the observed 17 cm of differential heave in the field (Walker et al., 2004). However, for this control simulation, we did not consider the effects of (i) secondary water transport through horizontal cracks in the mineral soil or (ii) drying of additional stored water in soil cracks, surface depressions and organic layers.

Shear cracking near the freezing front and lenticular structure caused by previous year's ice lenses cause secondary hydraulic activity (Ping et al., 2004). Observations in the field suggest that drying plays an important role in differential frost-heave development. During the thawed season, most depressions have standing water and saturated organic layers of up to 25 cm thick. These depressions and organic layers show little or no ice accumulation in the frozen season. It is therefore possible that potentially 12 cm of water froze in the nonsorted circles. Both explanations might work concurrently to develop the amount of differential ice accumulation found in the field.

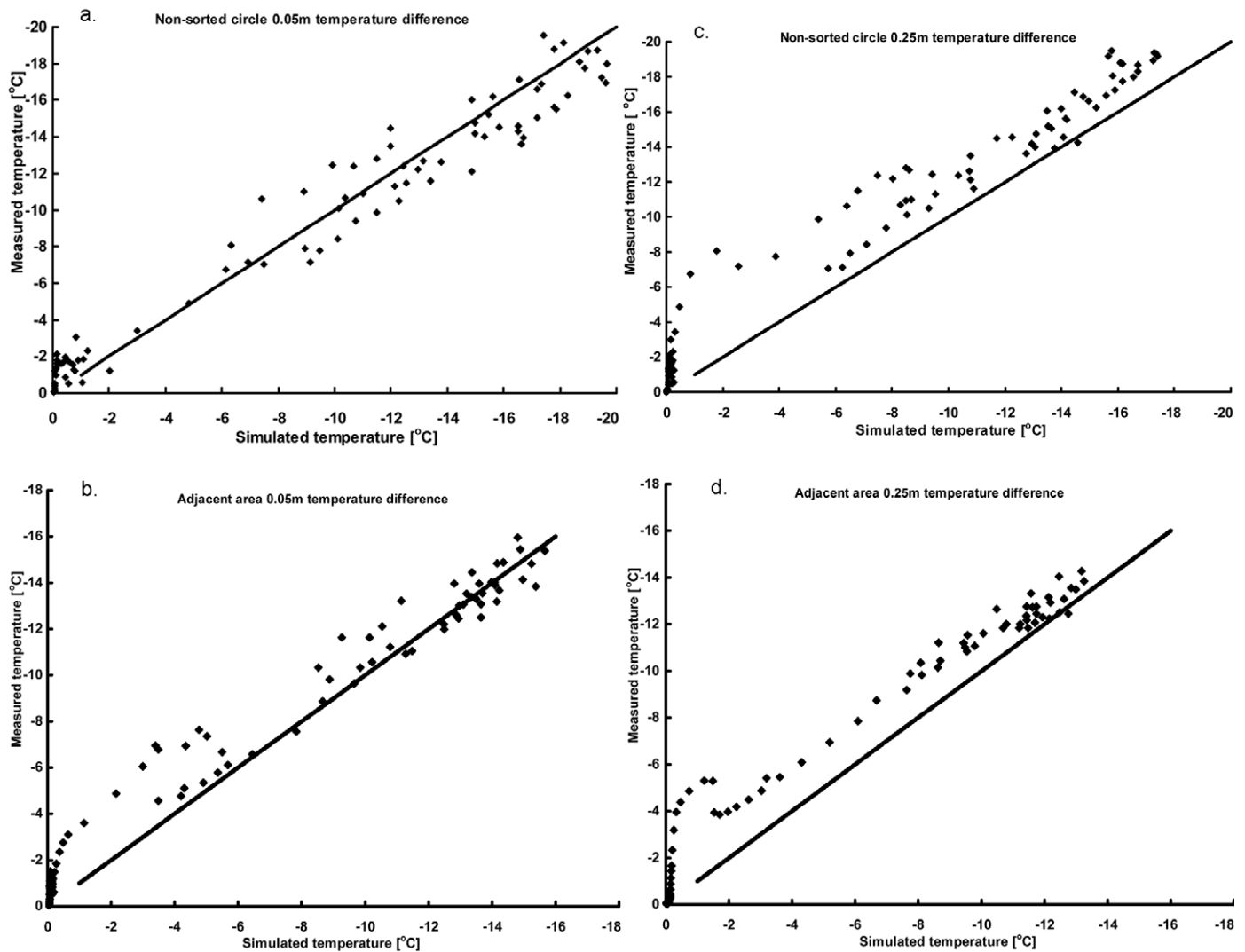


FIG. 10. Scattergrams of the measured and the simulated soil temperature (a) for the nonsorted circle at 5 cm depth, (b) for the adjacent tundra at 5 cm depth, (c) for the nonsorted circle at 25 cm depth, and (d) for the adjacent tundra at 25 cm depth.

Experiments

We used the model to simulate the effects of warming on the horizontal liquid-water movement in the active layer during freezing. The first simulated scenario was with a relative warming of the air temperature with respect to our control temperature, which resulted in a freezing rate reduction. Figure 11 shows the results of two levels of freezing rate reduction compared with the control freezing rate. It was found that a 10% freezing rate reduction leads to an 8% reduction of the horizontal liquid water movement, and a 20% freezing rate reduction leads to a 14% reduction in liquid water movement.

Slower changes in the air temperature reduce water movement; the soil has more time to cool overall, and local temperature gradients in the soil are limited. Less differential heave reduces root stress and promotes plant growth in the nonsorted circle. Additionally, a warmer soil temperature during the summer increases soil nutrient availability and the decomposition of soil organic matter (Epstein et al., 2001, 2000). Increases in growing season length over the last few decades (another by-product of climate change) may have also affected vegetation development (Hinzman et al., 2005). Together, these changes may alter the existing land surface conditions of the tundra. In

the future, we should address whether a warming climate trend does indeed affect the freezing rate with time, as used in this scenario. Climate records along a climate gradient from south to north do not suggest a change in freezing period characteristics (Daanen, 2006). At this point, not enough data are available to suggest changes in the freezing rate are indeed a side effect of current climate warming.

Summer warming increases nutrient availability (Chapin et al., 1995; Hartley et al., 1999; Schmidt et al., 2002), which promotes plant growth toward the center of the circle. Using WIT to simulate the effects of changing insulation at the soil surface, we find that 20 and 40% increases in the insulation of vegetated tundra lead to approximate increases of 10 and 30%, respectively, in the horizontal water movement from vegetated tundra to the nonsorted circle. These increases result in a stabilizing effect on the nonsorted circle ecosystem. A longer, warmer growing season for plants would make them more capable of establishing and growing in the center of the nonsorted circles; however, these plants need to overcome the additional heave on the circle generated by increased insulation in the adjacent tundra.

If the conditions are suitable enough for the plants to overcome frost heave on the nonsorted circle, then the process of

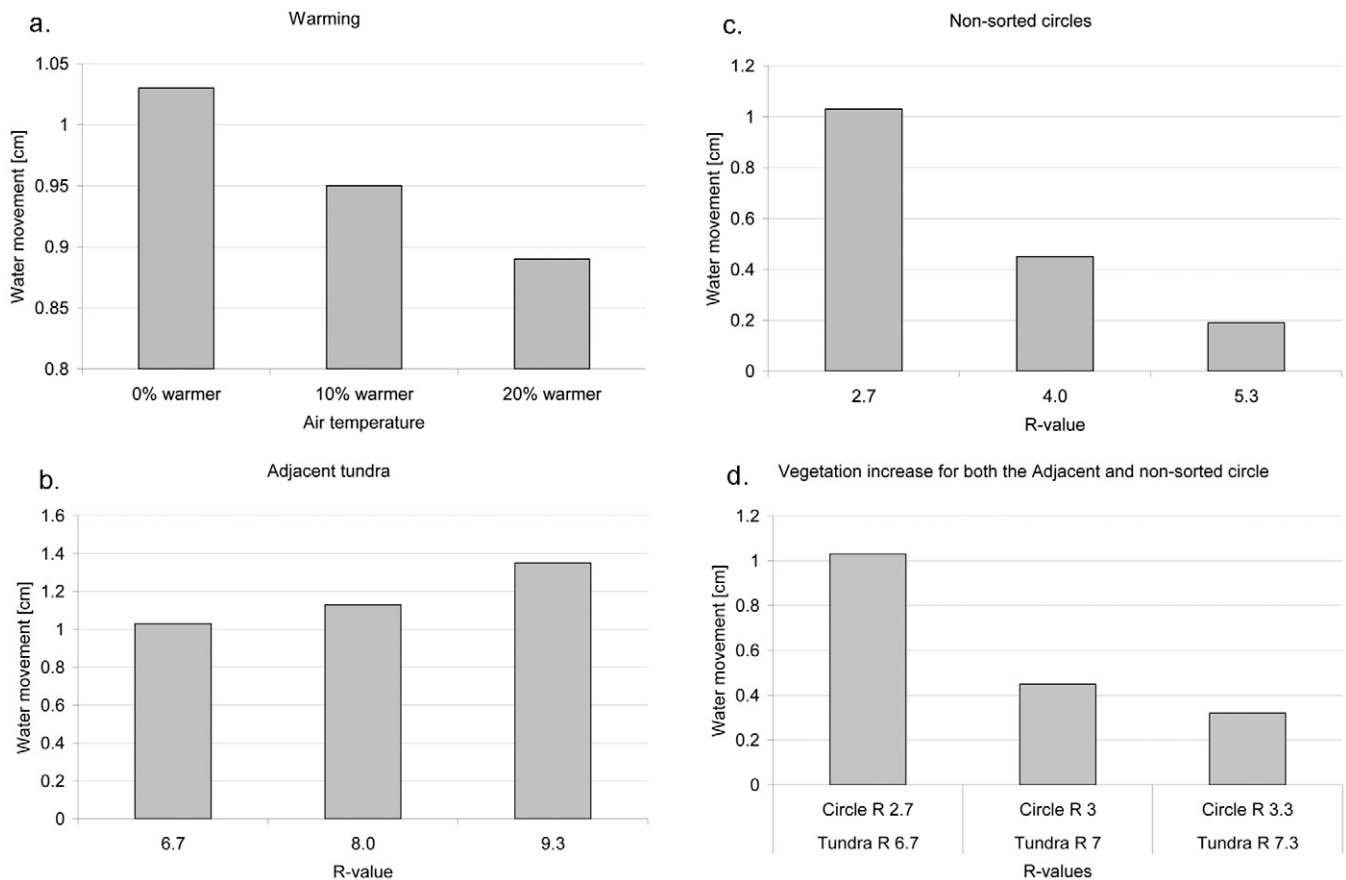


FIG. 11. (a) Effect of relative warming of the air temperature on the horizontal movement of liquid water during freezing. (b) Effect of increased vegetation, expressed in R-values ($\text{m}^2 \text{s } ^\circ\text{C J}^{-1}$), in the adjacent tundra on the horizontal movement of liquid water during freezing. (c) Effect of increased vegetation, expressed in R-values, on top of the nonsorted circle on the horizontal movement of liquid water during freezing. (d) Effect of even vegetation and snow increases, expressed in R-values, on the horizontal movement of liquid water during freezing.

heave degeneration might initiate. Figure 11c shows that 50 and 100% increases in the insulation on the nonsorted circle lead to 60 and 80% decreases, respectively, of the liquid water movement toward the nonsorted circle. This simulation result shows that insulation on the nonsorted circle can strongly affect the amount of water that can be attracted to the nonsorted circles, if the plants are able to colonize the entire bare surface of the nonsorted circle. If a part of the nonsorted circle remained without vegetation cover, it is likely that this part will experience more ice accumulation because more water is available from the larger adjacent tundra for heave in this small bare area.

Rather than an increase of vegetation in specific areas, it may be that the entire surface will experience denser vegetation and, due to increased winter precipitation, there will be an increase in the R-value for the entire ecosystem. Figure 11d shows that a combined increase in R-value ($\text{m}^2 \text{s } ^\circ\text{C J}^{-1}$) of 3 in insulation on the nonsorted circle and on adjacent tundra results in a 56% decrease in the horizontal liquid water flux. With an increase in the R-value of 6 in the boundary layer for the nonsorted circle and adjacent tundra, the horizontal liquid water flux reduces to 70%. This mathematical experiment shows that insulation of the nonsorted circle leads to a stronger response on the horizontal

water movement than increased insulation of the adjacent tundra.

In the final experiment, we simulated stress cracks (visible as lenticular structure in the soil profile), which renders substantial increase in the horizontal hydraulic conductivity. Figures

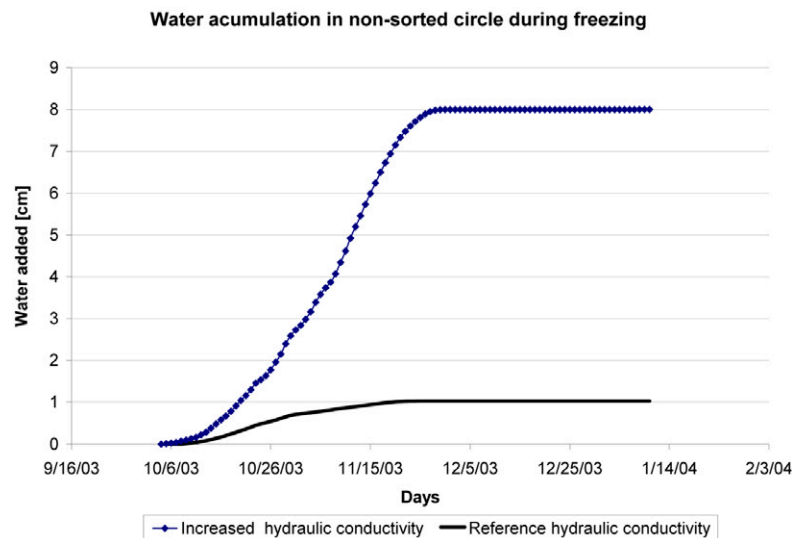


FIG. 12. Water accumulation in the nonsorted circle during the freezing period, using the reference ($1.0 \times 10^{-7} \text{ m s}^{-1}$) and an increased horizontal conductivity of $1.0 \times 10^{-5} \text{ m s}^{-1}$.

12 and 13 show the cumulative flux and the flux rate, respectively. Considerably more water (8 cm) can flow to the nonsorted circle during the freezing period when the horizontal hydraulic conductivity is 100 times greater than the vertical conductivity. We chose this value without any knowledge of the effects of the cracks on the hydraulic conductivity. The model, however, suggests that a larger value of the horizontal hydraulic conductivity can explain the behavior of the ecosystem better than a smaller value. If we compare our numbers with the soil used in Hansson et al. (2004), which is a Kanagawa sandy loam with a K_s of $3.2 \times 10^{-6} \text{ m s}^{-1}$, we can reasonably assume that our soil has a value of 10^{-5} m s^{-1} in the horizontal direction. The figures also show that the water flux depends on the temporal fluctuation of the air temperature, and that it increases with time as the liquid water in the active layer freezes, up to the point where ice accumulation reduces the hydraulic conductivity and the liquid water flux. Assuming this change in hydraulic conductivity is reasonable, the result of this experiment shows that WIT is capable of simulating a liquid water flux that approximately resembles the actual differential heave observed in the field.

Conclusions and Future Research

Through WIT, we simulated the hydrology of the nonsorted circle ecosystem suitably and predicted soil temperatures at different depths compared to those observed in the field. By simulating climate warming effects on the horizontal distribution of the total water, we observed the following:

- A decreased freezing rate reduces the horizontal movement of water in the soil during freezing.
- Increased insulation of the areas outside the nonsorted circle increases horizontal water flow toward the center of the circle.
- Increased insulation on the nonsorted circle during freezing strongly reduces the horizontal water movement toward the center of the circle.
- Insulation changes on nonsorted circles have a greater effect on horizontal water flow than insulation changes in adjacent tundra.

Vegetation response to climate warming is potentially a key factor controlling the movement of liquid water in the active layer during freezing. Processes responsible for the secondary frost heave are still under active research and not well understood. Our research sheds an initial light on possibility of higher horizontal fluid migration as a process of producing secondary frost heave.

ACKNOWLEDGMENTS

Financial support for this research from the Arctic Regions Supercomputing Center of the University of Alaska Fairbanks (UAF) is duly acknowledged. Field data used in this research were made available through a grant by the National Science Foundation OPP-0120736. The authors wish to acknowledge the personal support provided by Dr. Frank Williams, director, and Dr. Greg Newby, acting chief scientist, the Arctic Regions Supercomputing Center, UAF, and Dr. Vladimir Romanovsky, associate professor, Geophysical Institute, UAF. The comments received from the three anonymous reviewers and

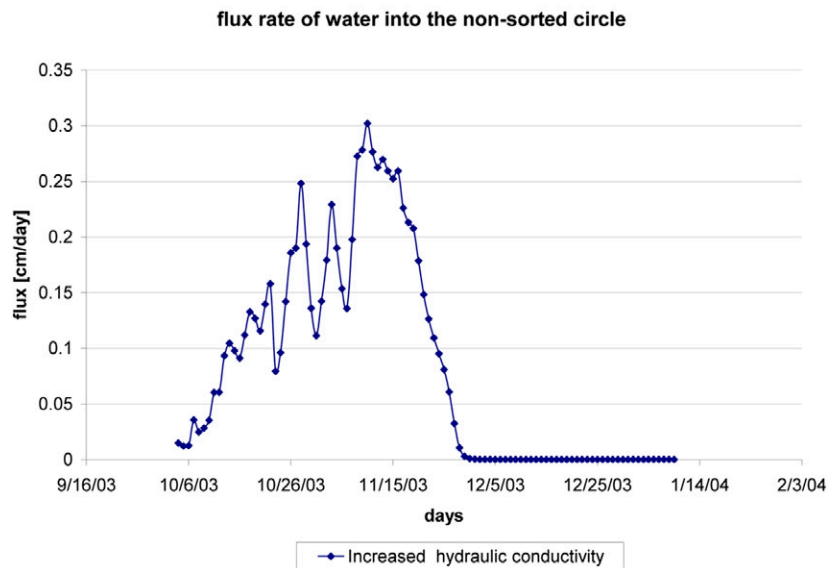


FIG. 13. Flux rate of water into the nonsorted circle (cm d^{-1}) for the increased horizontal conductivity case.

the associate editor, Dr. David DiCarlo has helped us immensely in improving the quality and content of this paper.

References

- Boike, J., O. Ippisch, and K. Roth. 2002. Thermal and hydrological dynamics of a mud boil: Any clues about its formation? *J. Geocryology Glaciology* 24:538–543.
- Celia, M.A., E.T. Bouloutas, and R.L. Zarba. 1990. A general mass-conservative numerical-solution for the unsaturated flow equation. *Water Resour. Res.* 26(7):1483–1496.
- Chapin, F.S., III, G.R. Shaver, A.E. Giblin, K.J. Nadelhoffer, and J.A. Laundre. 1995. Responses of arctic tundra to experimental and observed changes in climate. *Ecology* 76:694–711.
- Chapin, F.S., III, M. Sturm, M.C. Serreze, J.P. McFadden, J.R. Key, A.H. Lloyd, A.D. McGuire, T.S. Rupp, A.H. Lynch, J.P. Schimel, J. Beringer, W.L. Chapman, H.E. Epstein, E.S. Euskirchen, L.D. Hinzman, G. Jia, C.-L. Ping, K.D. Tape, C.D.C. Thompson, D.A. Walker, and J.M. Welker. 2005. Role of terrestrial ecosystem changes in arctic summer warming. *Science* 310:657–660.
- Daanen, R.P. 2004. Modeling liquid water flow in snow. PhD. diss. Univ. of Minnesota, Minneapolis.
- Daanen, R.P. 2006. Soil climate and vegetation along the North American Arctic Transect. Poster Presentation at the American Association for the Advancement of Science Arctic Division Annual Conf., Fairbanks, AK. 2–4 Oct. 2006.
- Epstein, H.E., F.S. Chapin, III, M.D. Walker, and A.M. Starfield. 2001. Analysing functional type concept in arctic plants using a dynamic vegetation model. *Oikos* 95:239–252.
- Epstein, H.E., M.D. Walker, F.S. Chapin, III, and A.M. Starfield. 2000. A transient, nutrient based model of arctic plant community response to climate warming. *Ecol. Appl.* 10:824–841.
- Fowler, A.C., and W.B. Krantz. 1994. A generalized secondary frost heave model. *SIAM J. Appl. Math.* 54:1650–1675.
- Hansson, K., J. Simunek, M. Mizoguchi, and L.-Ch. Lundin. 2004. Water flow and heat transport in frozen soil: Numerical solution and freeze–thaw applications. *Vadose Zone J.* 3:693–704.
- Hartley, A.E., C. Neill, J.M. Melillo, R. Crabtree, and F.P. Bowles. 1999. Plant performance and soil nitrogen mineralization in response to simulated climate change in subarctic dwarf shrub heath. *Oikos* 86:331–343.
- Hinzman, L.D., N.D. Bettez, W.R. Bolton, F.S. Chapin, M.B. Dyrgerov, C.L. Fastie, B. Griffith, R.D. Hollister, A. Hope, H.P. Huntington, A.M. Jensen, G.J. Jia, T. Jorgenson, D.L. Kane, D.R. Klein, G. Kofinas, A.H. Lynch, A.H. Lloyd, A.D. McGuire, F.E. Nelson, W.C. Oechel, T.E. Osterkamp, C.H. Racine, V.E. Romanovsky, R.S. Stone, D.A. Stow, M. Sturm, C.E.

- Tweedie, G.L. Vourlitis, M.D. Walker, D.A. Walker, P.J. Webber, J.M. Welker, K.S. Winker, K. Yoshikawa. 2005. Evidence and implications of recent climate change in northern Alaska and other arctic regions. *Clim. Change* 72(3):251–298.
- Ippisch, O. 2003. Coupled transport in natural porous media. Ph.D. diss. Univ. of Heidelberg, Germany.
- Jia, G.J., H.E. Epstein, and D.A. Walker. 2003. Greening of the Alaskan Arctic over the past two decades. *Geophys. Res. Lett.* 30(20):2067, doi:10.1029/2003GL018268.
- Kay, B.D., and P.H. Groenevelt. 1974. On the interaction of water and heat transport in frozen and unfrozen soils: I. Basic theory, the vapor phase. *Soil Sci. Soc. Am. Proc.* 38:395–400.
- Kung, S.K.J., and T.S. Steenhuis. 1986. Heat and moisture transfer in a partly frozen nonheaving soil. *Soil Sci. Soc. Am. J.* 50(5):1114–1122.
- Liebenthal, C., and T. Foken. 2007. Evaluation of six parameterization approaches for the ground heat flux. *Theor. Appl. Clim.* 88(1–2):43–56.
- Maxwell, B. 1992. Arctic climate: Potential for change under global warming. p. 11–34. *In* F.S. Chapin, R.L. Jeffries, J.F. Reynolds, G.R. Shaver, and J. Svoboda (ed.) *Arctic ecosystems in a changing climate. An ecophysiological perspective.* Academic Press, San Diego, CA.
- Miller, R.D. 1980. Freezing phenomena in soil. p. 254–299. *In* D. Hillel (ed.) *Applications of soil physics.* Academic Press, New York.
- Misra, D. 1994. Mixed finite element analysis of one-dimensional heterogeneous Darcy flow. Ph.D. diss. University of Minnesota, Minneapolis.
- Mitchell, J.K. 1993 *Fundamentals of soil behavior.* John Wiley & Sons, New York.
- Myneni, R.B., C.D. Keeling, C.J. Tucker, G. Asar, and R.R. Nemani. 1997. Increased plant growth in the northern high latitudes from 1981 to 1991. *Nature* 386:698–702.
- Nicolosky, D.J., G.S. Tipenko, and V.E. Romanovsky. 2004. A coupled thermo-mechanical model of the differential frost heave. *EOS Trans. AGU*, 85(47), Fall Meet. Suppl., Abstract C13-B-0282.
- O'Neill, K., and R.D. Miller. 1985. Exploration of a rigid ice model of frost heave. *Water Resour. Res.* 21:281–296.
- Peterson, R.A., and W.B. Krantz. 2003. A mechanism for differential frost heave and its implications for patterned ground formation. *J. Glaciology* 49(164):69–80.
- Ping, C.L., T.M. Jorgeson, and Y. Shur. 2004. Soil cryogenic structures and their implications for land use in Alaska. *J. Glaciology Geocryology* 26:1–7.
- Richards, L.A. 1931. Capillary conduction of liquids through porous medium. *Physics* 1:318–333.
- Schmidt, I.K., S. Jonasson, G.R. Shaver, A. Michelsen, and A. Nordin. 2002. Mineralization and distribution of nutrients in plants and microbes in four arctic ecosystems: Responses to warming. *Plant Soil* 242:93–106.
- Spaans, E.J.A., and J.M. Baker. 1996. The soil freezing characteristic: Its measurement and similarity to the soil moisture characteristic. *Soil Sci. Soc. Am. J.* 60:13–19.
- Tape, K., M. Sturm, and C. Racine. 2006. The evidence for shrub expansion in northern Alaska and the Pan-Arctic. *Glob. Change Biol.* 12:686–702.
- van Genuchten, M.Th. 1980. A closed form equation for predicting the hydraulic conductivity of unsaturated soil. *Soil Sci. Soc. Am. J.* 44:892–898.
- Walker, D.A., H.E. Epstein, W.A. Gould, A.M. Kelley, A.N. Kade, J.A. Knudson, W.B. Krantz, G. Michaleson, R.A. Peterson, C.L. Ping, M.A. Reynolds, V.E. Romanovsky, and Y. Shur. 2004. Frost-boil ecosystems: Complex interactions between landforms, soils, vegetation, and climate. *Permafrost Periglacial Processes* 15:171–188.
- Walker, M., H. Wahren, L. Ahlquist, J. Alatolo, S. Bret-Harte, M. Calef, T. Callaghan, A. Carroll, C. Copass, H. Epstein, G. Henry, R. Hollister, I.S. Jonsdottir, J. Klein, B. Magnusson, U. Molau, S. Oberbauer, S. Rewa, C. Robinson, G. Shaver, K. Suding, A. Tolvanen, Ø. Totland, P.L. Turner, C. Tweedie, P. Webber, and P. Wookey. 2006. Plant community response to experimental warming across the tundra biome. *Proc. Natl. Acad. Sci. USA* 103:1342–1346.
- Walsh, J.E. 1993. The elusive Arctic warming. *Nature* 361(6410):300–301.
- Washburn, A.L. 1956. Classification of patterned ground and review of suggested origins. *Geol. Soc. Am. Bull.* 67:823–866.